Digest Journal of Nanomaterials and Biostructures Vol. 8, No. 2, April - June 2013, p. 765 - 775

FACILE SYNTHESIS OF IRON OXIDE, IRON-COBALT AND ZERO VALENT IRON NANOPARTICLES AND EVALUATION OF THEIR ANTI MICROBIAL ACTIVITY, FREE RADICLE SCAVENGINGING ACTIVITY AND ANTIOXIDANT ASSAY

NARENDHAR CHANDRASEKAR*, K.MURUGU MOHAN KUMAR[a], KARPANAI SELVAN BALASUBRAMNIAN[b], KARUNAMURTHY.K [c], RUBAL VARADHARAJAN[d]
Department of Nanotechnology, Sri Ramakrishna Engineering College, Coimbatore, India
[a]*Pavendhar Bharathidasan College of Engineering and Technology, Tiruchirappalli, India*
[b]*Department of Biotechnology, Anna University of Technology, Tiruchirappalli, India*
[c]*Department of Mechanical Engineering, CARE School of Engineering, Tiruchirappalli, India*
[d]*Department of Materials Science and Engineering, CARE School of Engineering, Tiruchirappalli, India*

Iron oxide, iron-cobalt core shell nanoparticle and zero valent iron nanoparticles were synthesized by a one pot, room temperature method using co-precipitation, micro emulsion and wet chemical method using gallic acid as the surfactant and reducing agent. The properties and distribution of the particles were confirmed by UV-Visible spectroscopy, dynamic light scattering (DLS) analysis and Scanning Electron Microscopy (SEM). The stability of the particles were evaluated by observation for visible aggregates over a weeks period and progressed for further studies. In this report the anti microbial activities of three different forms of iron namely iron oxide, iron-cobalt composite and zero valent iron were evaluated by zone of inhibition studies by agar well diffusion method on multi drug resistant *Staphylococcus aureus sp.* The drug kanamycin an amino glycoside antibiotic was used as the positive control for the comparison of the antimicrobial activity. The incubation period of the evaluated microbial inhibition assay was 12 hours from the time on inoculation and well assay. During repeated trials the zone of inhibition remained at high areas proving the particles are toxic to the microbes.

(Received February 12, 2013: Accepted May 7, 2013)

Keywords: Core shell nanoparticles, Dynamic Light Scattering, Transmission electron microscopy, Zone of Inhibition and antimicrobial activity

1. Introduction

Nanoparticles are distinct materials with the entire or a part of the structure having submicron dimension, preferably in the range of 1-100 nm. Iron oxide and zero valent nanoparticles have long been used for the antimicrobial activities for medical procedures, storage and use of food materials. The use of these metals for antimicrobial activities has been proved effectively in medical field for anti microbial surgical tools, dressings and wound healing patches. The progressive analysis of surfactant dependent antimicrobial activities have given an in depth view of the properties of nanoparticles according to their size and concentration of surfactant used.

*Corresponding author: narendhar.nano@gmail.com

Although the antimicrobial uses of metals have largely been supplemented by the use of antibiotics (1, 2). This study is concentrated on the various synthetic routes of Iron nanoparticles and their anti microbial activity dependant on the various factors like shape of the particles surfactants used. Plant mediated biosynthesis of nanoparticles have been of recent interest for the researchers to exploit the wasted or recycled biomass for the synthetic application. (5, 6 and 7) and micro organisms (8, 9) the ultimate effect of the nanosized material is to be employed in fabrication of antimicrobial patch. Anti Oxidant assay was performed by phosphomolebdenum method
Gallic acid also known as 3, 4, 5-trihydroxybenzoic acid and exists in minute quantity in nutgalls. It exists as a product of the decomposition of tannin, a naturally occurring polyphenol. They exhibit anti fungal, anti-viral properties and antibacterial properties of their own which was the motivation for its use over the other reducing agents and stabilizers. It acts as an antioxidant and helps to protect our cells against oxidative damage and was found to show cytotoxicity against cancer cells, without harming healthy cells. For the synthesis of nanoparticles gallic acid has been utilized so far for individual metals (10, 11). This will be the first time commercially available gallic acid has been employed to synthesize a core shell structure and evaluated for antimicrobial activity.

2. Materials Used

Ferrous sulphate, Ferric chloride, gallic acid, cobalt acetate and toluene were purchased from Loba Chemie and used without further purification. All other reagents were purchased from Merck India and used without further purification. For all the experiments 18 $m\Omega/cm^2$ millipore water was used.

3. Methods Of Synthesis

3.1 Wet Chemical Method

Initially the solutions of ferrous sulphate 0.5 M and ferric chloride 1M was prepared in 100 ml of millipore water and stirred for ten minutes. 1 mM molar solution of gallic acid was prepared and stored at room temperature. This solution was stirred for 24 hours for removing any ionic impurities and to allow the entire precursor ions to be reduced. All the samples were confirmed by UV-Visible spectroscopy for absorption maxima and then checked over a week's period for stability in the peak shift.

All the synthesized particles were filtered twice with Whatman filter paper before taking UV Visible spectroscopy and stored to evaluate the stability. After verifying the peak shifts in the UV-Visible spectroscopy again the particles were centrifuged at 8000 rpm at room temperature for 30 minutes. Supernatant was discarded and the residue was washed with Millipore water and centrifuged again. This process was repeated for two more times for removing any ionic impurities so they do not interfere with the toxicity of the particles to the microorganisms.

3.2 Reverse Micelle

In this method the water in oil micro emulsion was adopted (23, 26). The emulsion used was created by using toluene as the continuous phase and water as the stationary phase. The metal precursors ferrous sulphate 0.2mM and cobalt acetate 0.1mM were prepared by using Millipore water and stored. Sodium do decyl sulphate 1% (W/V) was added to toluene and stirred for 15 minutes.

1mM of Gallic acid 50ml in millipore water in toluene and 50ml each of the metal precursor solutions are added suddenly to toluene and homogenized at 5000 rpm for ten minutes. The resultant color change indicates the formation of the nanoparticles. The schematic of the reverse micelle is given in the figure 1.

3.3 Zero Valant Iron Nanoparticle Synthesis

For the synthesis of Zero valent iron nanoparticles ferrous sulphate 0.1mM was prepared in 10 ml Millipore water and mixed with 90ml of ethanol. To this mixture 5 ml of 1mM gallic acid solution was added and the resultant solution was stirred for 24 hours for complete reduction of the particles.

The color of the solution changed over a period of time and UV-Visible spectra was taken to confirm the formation of particles. The resulting nanoparticles' suspensions were filtered twice using Whatman filter paper. All the particles were checked for stability over a period of time and analyzed for time dependant shift in UV Visible spectroscopy.

3.4 Reverse Micelle Synthesis

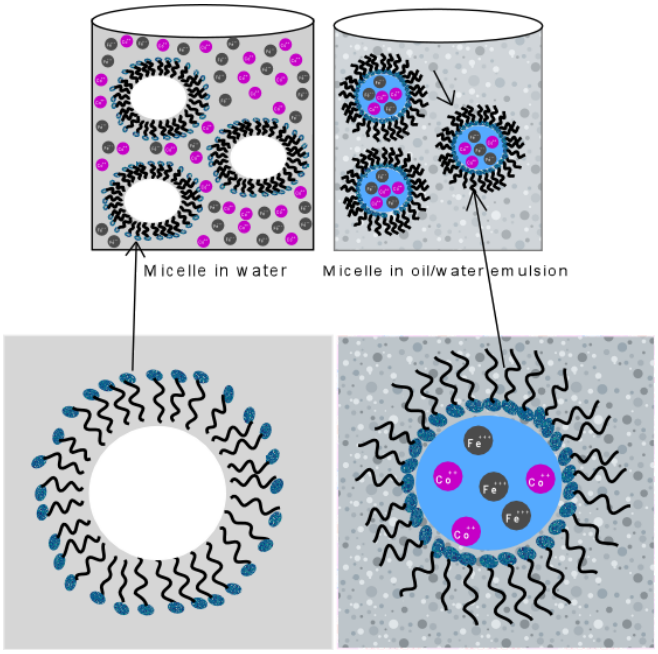

Fig.1. Schematic of Gallic acid micelles.

4. Antioxidant Activity - DPPH Radical Scavenging Activity

Different volumes of extracts were taken in different test tubes. The volume was adjusted to 100 µl with methanol and 5 mL of 0.1 mMmethanolic solution of DPPH● was added to these tubes, and then shaken vigorously. The tubes were allowed to stand for 20 min at 27ºC in dark at room temperature. The control was prepared as above without any extract. The absorbances of the samples were measured at 517 nm (Blios, 1958), using a spectrophotometer (Model-Hitachi U-2000). The antioxidant capacities of the samples using DPPH assay were compared with those of BHA, BHT, Rutin and quercetin and the blank. Radical scavenging activity was expressed as the inhibition percentage of free radicals by the samples and was calculated using the following formula.

% radical scavenging activity = (Control OD-Sample OD/Control OD) ×100

5. Chelating capacity

Reducing power assay

Various concentrations of Ethyl acetate extract of stem (1ml) were mixed with 2.5 ml of 1% sodium phosphate buffer (pH 6.6) and 2.5 ml of 1% potassium ferricyanide. Then the mixture

was incubated at 50°C for 30 min. After 2.5 ml of 10% TCA were added to the mixture was centrifuged at 3,000 rpm for 10 min. The upper layer (2.5 ml) was mixed with 2.5 ml deionized water with 0.5 ml of 0.1% of ferric chloride and the absorbance was measured at 700 nm. The assays were carried out in triplicate and the results were expressed as mean values ± SD. Ascorbic acid was used as a standard.

6. Phosphomolybdenum Assay

The antioxidant activity of samples was evaluated by the phosphomolybdenum method (Prieto*et al.,* 1999). An aliquot of 50 µl of sample solution (1 mM in dimethyl sulphoxide) was combined in a 4 mL vial with 1 mL of reagent solution (0.6 M sulphuric acid, 28 mM sodium phosphate and 4 mM ammonium molybdate). The vials were capped and incubated in a water bath at 95 0C for 90 min. After the samples had cooled to room temperature, the absorbance of the mixture was measured at 765 nm against a blank. The results reported are mean values expressed as grams of ascorbic acid equivalents per gram sample (AEAC).

7. Results and discussion

The synthesized samples were dried and redispersed in ethanol for UV-Visible spectroscopy, dynamic light scattering and SEM analysis.

7.1 Uv-Visible Spectroscopy

The synthesized samples were washed in Millipore water and dispersed in ethanol for UV-Visible spectroscopy analysis. The analysis was done using JASSCO-V 650 UV-Visible Spectrometer. The samples showed characteristic peak in the range of 580 nm for iron cobalt, 675 nm for iron oxide and 328 nm for zero valent iron nanoparticles.

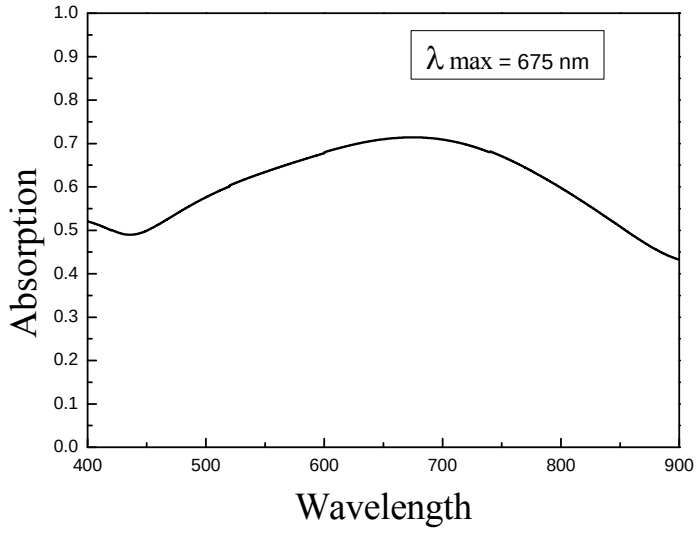

Fig.. 2. UV-Visible Spectroscopy analysis of iron oxide nanoparticles

The particles were analysed and the resultant peak 675 nm existed at the range typical to the peak of iron oxide nanoparticles.

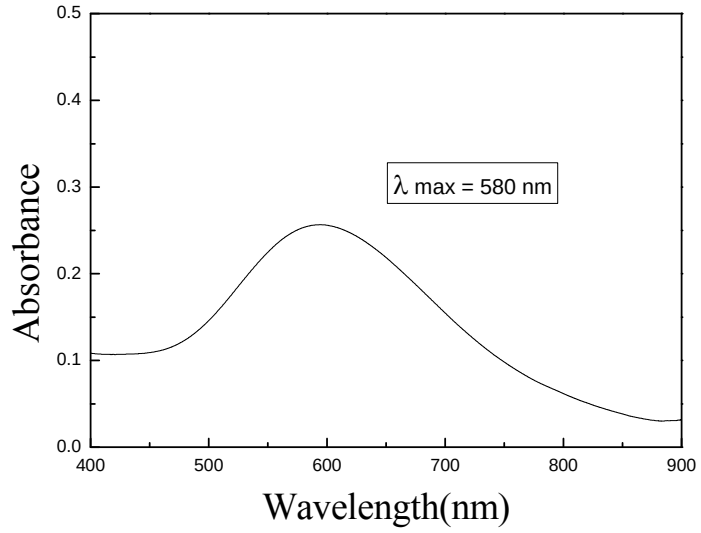

Fig. 3. UV-Visible Spectroscopy analysis of iron-cobalt nanoparticles.

The particles were analysed and the resultant peak at 580 nm existed at the range typical to the peak of iron based nanoparticles.

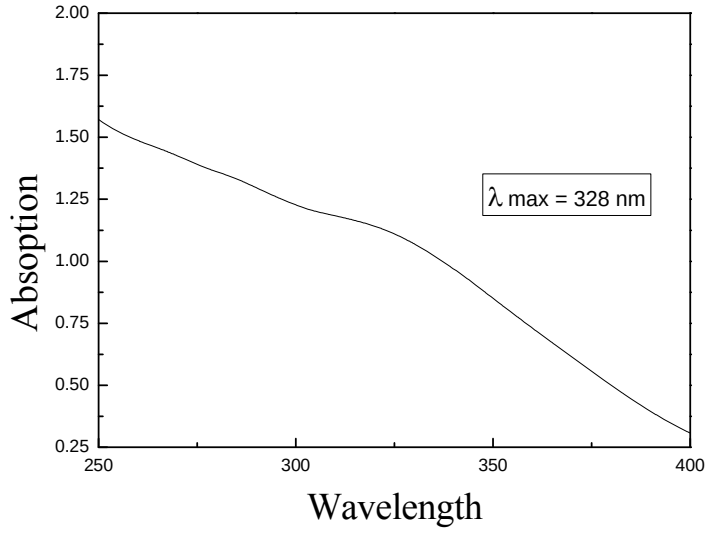

Fig.4. UV-Visible Spectroscopy analysis of zero valent iron nanoparticles.

The particles were analysed and the resultant peak existed at the range 328 nm typical to the peak of zerovalent iron nanoparticles.

The size and shape of the synthesized iron oxide nanoparticles was determined using **JEOL JSM 6701 f** Field Emission Scanning Electron Microscope (FESEM) operating at 3 kV accelrtation voltage at 19,000x magnification. The width of the area in focus was 7.7 mm which was chosen as the area where the maximum distribution of particles were seen.

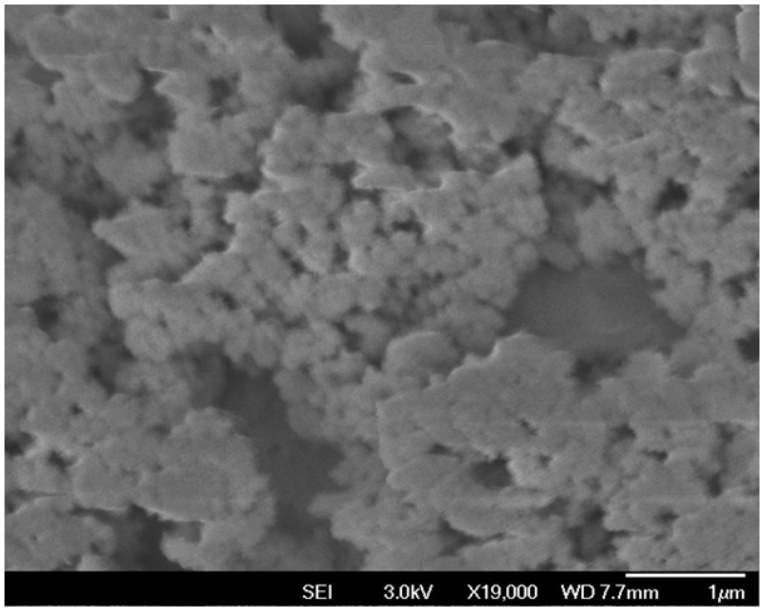

Fig.5. SEM analysis of Iron-Cobalt nanoparticles scale bar 1μm.

The scanning electron microscopy results of the iron oxide nanoparticle show that the multi particle aggregates are formed post synthesis. These can be due to the denaturation and aggregation during the sputtering process. As the temperature raises the chitosan polymer aggregates and forms micron sized aggregates. This can be avoided by use of the calcination process where the polymer is completely evaporated and only the iron particles remain. This will eliminate the possibility of encapsulation of the drug into the matrix of the polymer.

7.2 Dynamic Light Scattering

The size distribution of the particles in the solution form was analyzed using a Microtrac-Bluetrac particle size analyzer using a MALVERN ZETA SIZER. The stability of the particles were proved to be good as the zeta potential existed in the -23 mv range.

		Mean (mV)	Area (%)	Width (mV)
Zeta Potential (mV): -23.9	Peak 1:	-23.9	100.0	6.94
Zeta Deviation (mV): 6.94	Peak 2:	0.00	0.0	0.00
Conductivity (mS/cm): 1.11	Peak 3:	0.00	0.0	0.00
Result quality : Good				

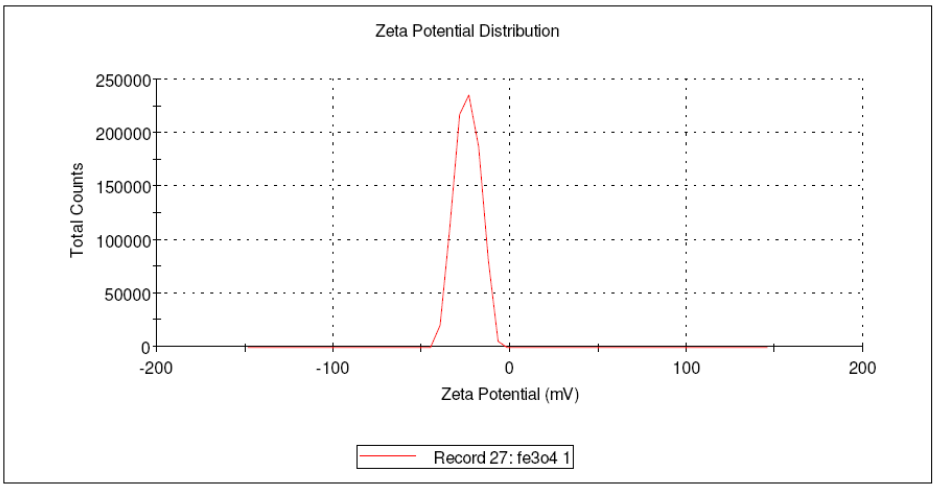

Fig. 6. Zeta potential of analysis of Iron oxide nanoparticles

		Diam. (nm)	% Intensity	Width (nm)
Z-Average (d.nm): 340.6	Peak 1:	239.2	100.0	52.88
PdI: 0.423	Peak 2:	0.000	0.0	0.000
Intercept: 0.967	Peak 3:	0.000	0.0	0.000

Result quality : Refer to quality report

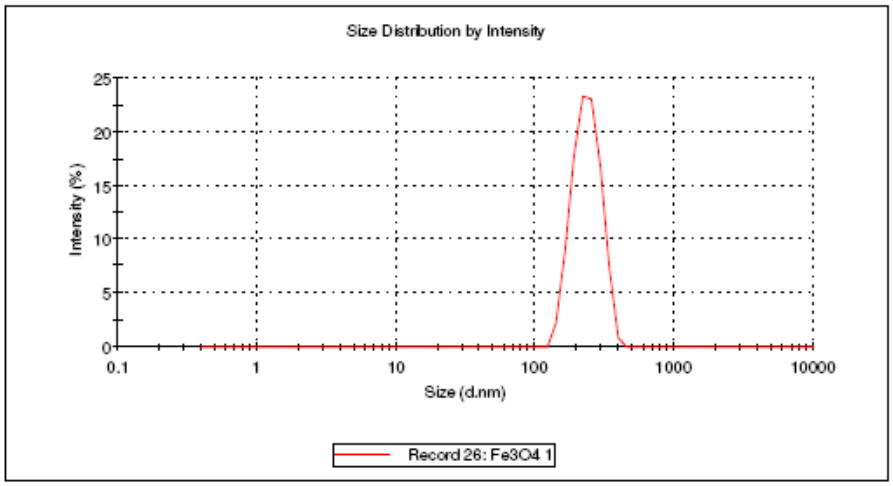

Fig. 7. Dynamic light scattering analysis of Iron oxide nanoparticles.

The zeta potential of the nanoparticles give an idea about the stability in the medium it is dispersed in. The nanoparticles in this case are suspend3ed in distilled Millipore water. If the potential exists in the +30 to -30 milli volts range the particle is said to be stable. We have all the three particles in the mentioned range which conclude that they are not aggregating and are stable in the conditions in which they are to be used. The iron oxide nanoparticles have the size of 239 nm as the average, the core shell nanoparticles, iron – cobalt have a mean diameter of 439 nm and the zerovalent iron nanoparticles have a mean diameter of 472 nm.

		Mean (mV)	Area (%)	Width (mV)
Zeta Potential (mV): -25.5	Peak 1:	-25.5	100.0	8.08
Zeta Deviation (mV): 8.08	Peak 2:	0.00	0.0	0.00
Conductivity (mS/cm): 0.899	Peak 3:	0.00	0.0	0.00

Result quality : Good

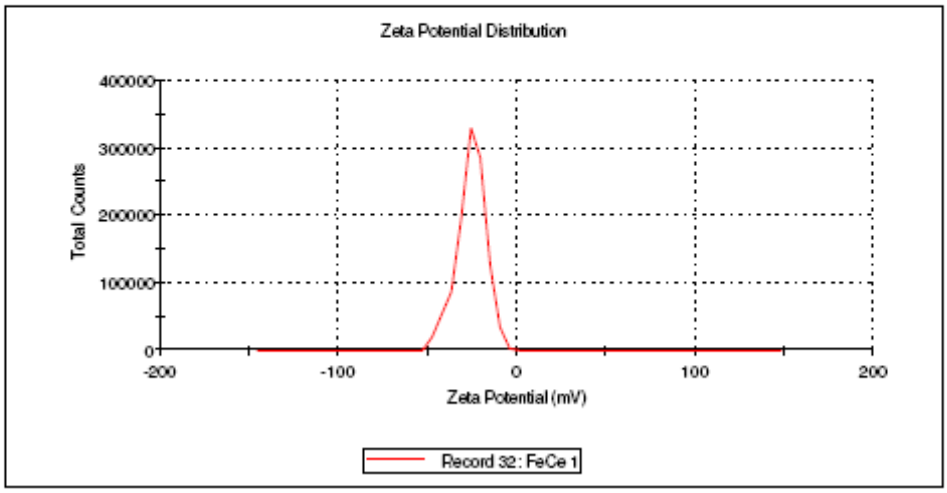

Fig. 8. Zeta potential of analysis of Iron cobalt nanoparticles

		Diam. (nm)	% Intensity	Width (nm)
Z-Average (d.nm): 454.2	Peak 1:	456.3	100.0	126.8
PdI: 0.222	Peak 2:	0.000	0.0	0.000
Intercept: 0.938	Peak 3:	0.000	0.0	0.000

Result quality : Good

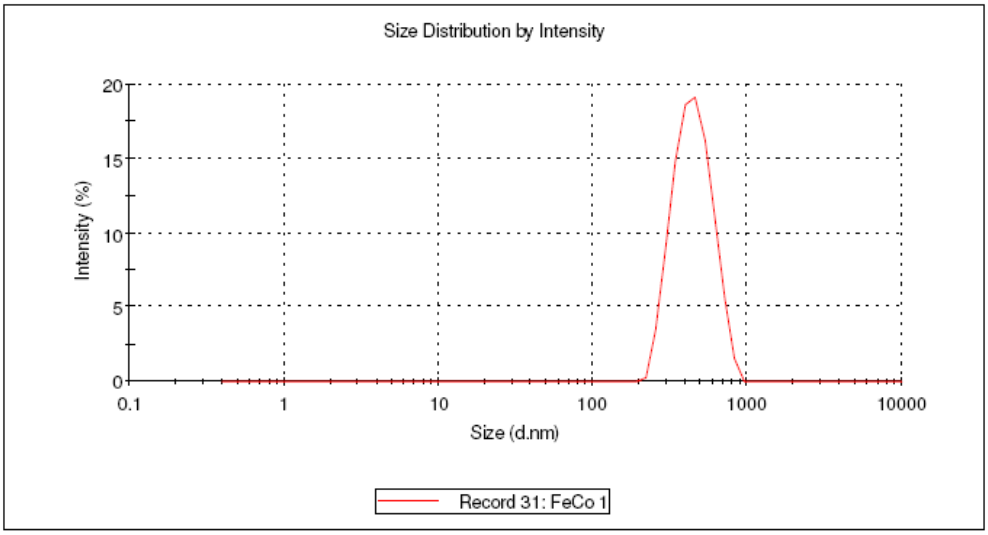

Fig. 9. Dynamic light scattering analysis of Iron cobalt nanoparticles.

		Mean (mV)	Area (%)	Width (mV)
Zeta Potential (mV): -28.0	Peak 1:	-22.7	71.7	6.47
Zeta Deviation (mV): 11.4	Peak 2:	-43.2	28.3	5.83
Conductivity (mS/cm): 0.523	Peak 3:	0.00	0.0	0.00

Result quality : Good

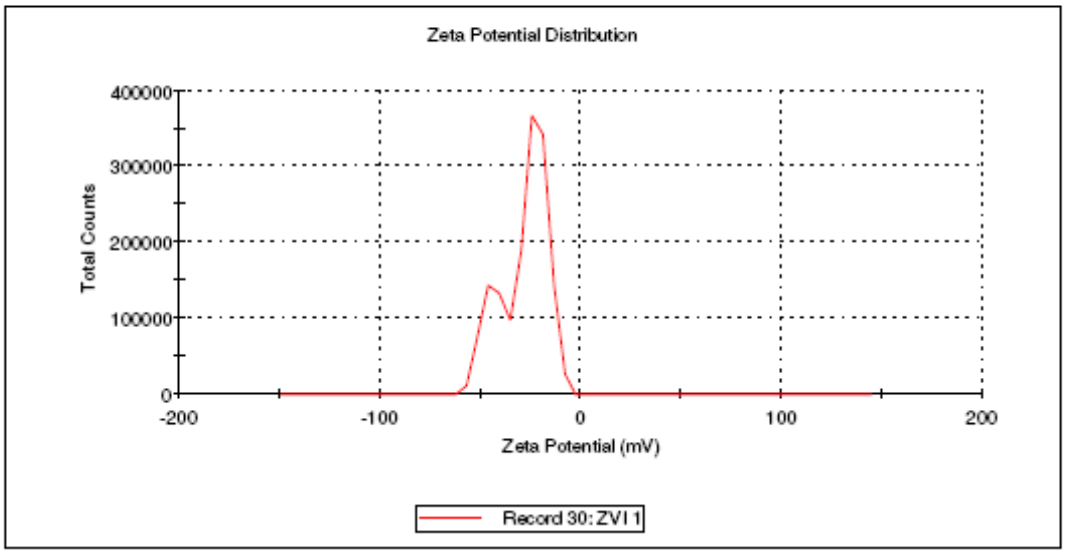

Fig. 10. Zeta potential of analysis of Zerovalent Iron nanoparticles

		Diam. (nm)	% Intensity	Width (nm)
Z-Average (d.nm): 472.0	Peak 1:	487.2	97.1	189.1
PdI: 0.233	Peak 2:	5189	2.9	481.0
Intercept: 0.909	Peak 3:	0.000	0.0	0.000

Result quality : Good

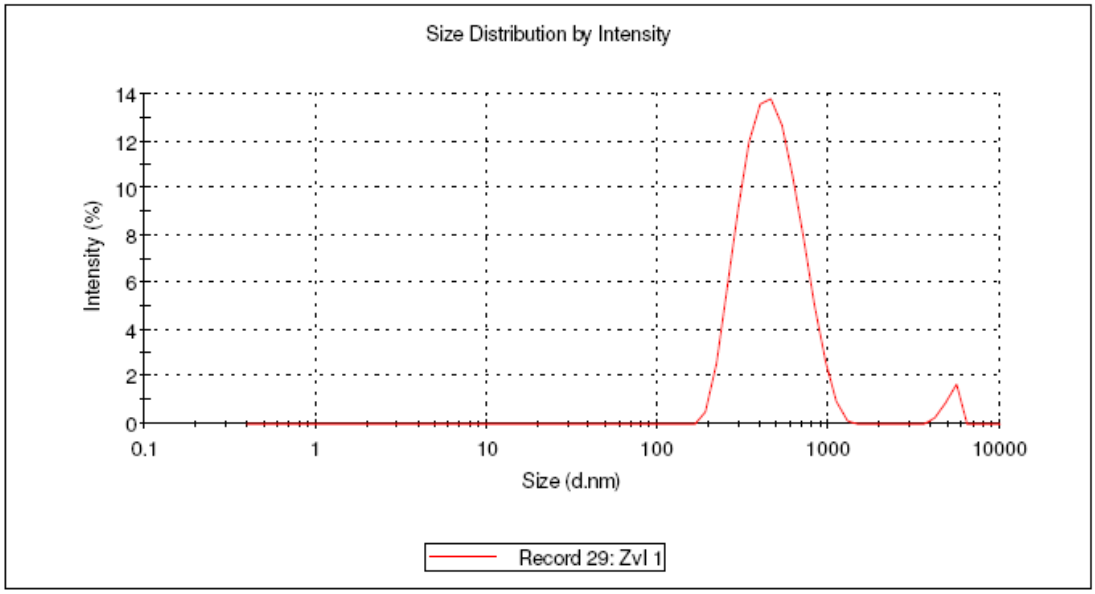

Fig. 11. Dynamic light scattering analysis of Zerovalent Iron nanoparticles

7.3 Antimicrobial Assay

The synthesized particles were evaluated for antimicrobial assays using *Staphylococcus aureus sp*. The nanoparticles were dried using a vacuum dessicator and 100 mg of the particles were suspended in 100 ml of distilled water i.e. 1% weight/volume . 40 µl of the synthesized particles were transferred to the microbe inoculated media after creating a well using a gel punch. The same quantity of particles was used for all the analysis.

Fig. 12. Zone of inhibition of particles synthesized by wet chemical method.
Index: Top left - iron oxide nanoparticles, Bottom left Iron-Cobalt nanoparticles and bottom right – Zero valent nanoparticles

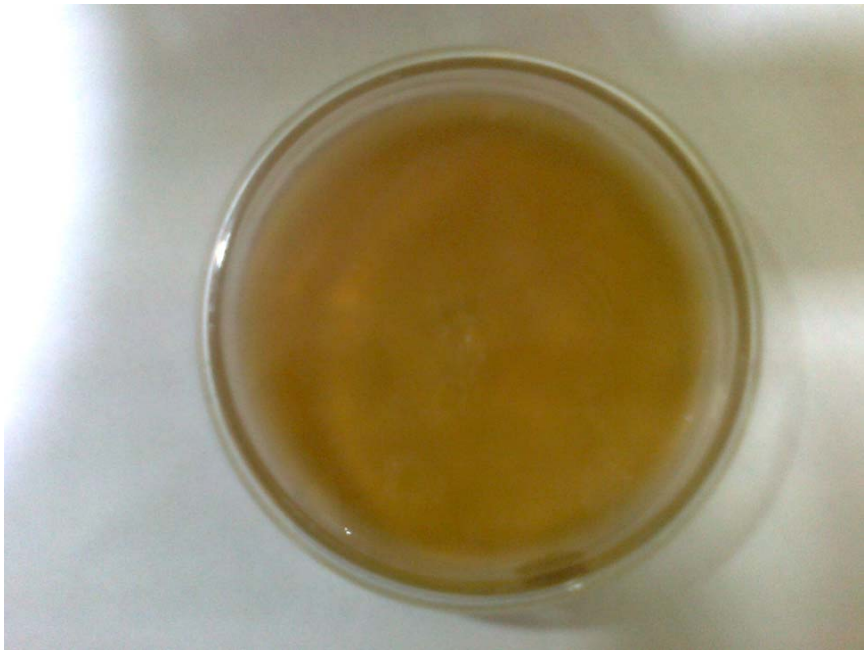

Fig. 13. Control plate with no drug or nanoparticles for evaluation of growth of microbes in the media Index: Top left - iron oxide nanoparticles, Zero valent iron nanoparticles

All the nanoparticles showed a good antimicrobial activity which was visible from the zones of inhibition of the nanoparticles in the agar media where the bacteria was grown.

Index of analysis

A- Control Liquid sample B- Zero valent Fe nanoparticle C- Iron Oxide nanoparticle

DPPH assay

Concentration	A	B	C
Control	1.0313	1.0349	1.1797
20µg	1.0177	0.9897	1.0371
40 µg	1.0110	0.9724	1.0371
60 µg	0.9952	0.9468	1.0251
80 µg	0.9949	0.8795	1.0213
100 µg	0.9698	0.8670	1.0178

Chelating assay

Concentration(µg)	A	B	C
50	2.8148	1.5056	1.4118
100	3.6102	1.6631	1.4618
200	4.8775	2.0192	1.7512
400	5.1015	2.1040	2.0460
800	10.0000	2.3053	2.9282

Phosphomolybdenum assay

Concentration(µg)	Control	A	B
50	0.0509	0.0619	0.0473
100	0.3747	0.0974	0.0544
200	0.4666	0.1895	0.0642
400	0.8464	0.3333	0.0944
800	2.9575	0.4210	0.1471

8. Conclusion

All the synthesized samples were characterized by UV Visible spectroscopy, dynamic light scattering and scanning electron microscopy to find the particle size. The particles synthesized by wet chemical method showed more zone of inhibition due to the presence of gallic acid which showed anti microbial activity of its own. The synthetic technique using gallic acid as a reducing agent and surfactant has not been reported so far for micro emulsion method and it was proved to be an easy way to synthesize nano dispersions without too much constraints. The samples of iron oxide and zero valent iron were subjected to anti oxidant assay had same activity of chelation with increasing concentration. The free radical scavenging was performed with the same results. The decrease in the activities could be due to the competitive inhibition due to high concentration of the contents present in the media which can reduce the surface area of the nanoparticles due aggregation of the crystals. As the size increases the surface area to volume ratio decreases which probably results in the reduced free radical scavenging and anti oxidant activity.

References

[1] M. Halwani1, Journal of Antimicrobial Chemotherapy **62**, 1291 (2008).
[2] Sukdeb Pal, Applied and Environmental Microbiology, Mar. 2007, p. 1712.
[3] Changha Lee, *Environ Sci Technol*. July 1; **42**(13), 49273 (2008).
[4] Bhupendra Chudasama, Nano Res **2**, 955 (2009).
[5] D. Jain Dig J Nanomater Bios, **4**(3), 557 (2009).
[6] Colleen M. Santoro, Nanobiotechnol **3**, 55 (2007).
[7] Jae Yong Song, Bioprocess Biosyst Eng **33**, 159 (2010).
[8] S.Anil Kumar, Biotechnol Lett **29**, 439 (2007).
[9] R. Varshney, Digest Journal of Nanomaterials and Biostructures **4**(2), 349 (2009). Wenxing Wang, J.colsurfa.2006.12.037
[10] S. A. Moreno-A lvarez, J Nanopart Res. 10.1007/s11051-010-0060
[11] R. Herrera-Becerra, Appl Phys A **100,** 453 (2010).
[12] Debanjan Guin, Materials Letters **62**, 3139 (2008).
[13] Deepak B Akolekar, Journal of Molecular Catalysis A: Chemical **238**, 78 (2005)
[14] Y.Ahn, Rev.Adv.Mater.Sci. **5,** 477 (2003).
[15] Onur Doker, Rev.Adv.Mater.Sci.**5,** 498 (2003).
[16] D. Predoi, Digest Journal of Nanomaterials and Biostructures **2**(1), 169 (2007).
[17] Marie-Paule Pileni, nature materials, VOL 2, MARCH 2003.
[18] N. Yildirim, Digest Journal of Nanomaterials and Biostructures **5**(4), 821 (2010).
[19] Candace T. Seip, NanoStructured Materials, **12**, 183 (1999).
[20] Sangaraju Shanmugam, Materials Chemistry and Physics **95**, 51 (2006).
[21] Jung Sun Kim, Nanomedicine: Nanotechnology, Biology, and Medicine **3**, 95 (2007).
[22] G. Hota, Colloids and Surfaces A: Physicochem. Eng. Aspects **232**, 119 (2004)
[23] Lei Qian, Colloids and Surfaces A: Physicochem. Eng. Aspects **260**, 79 (2005).
[24] C.T. Fleaca, Applied Surface Science **255**, 5386 (2009)
[25] Xiaoan Fu, Colloids and Surfaces A: Physicochemical and Engineering Aspects **179,** 65 (2001).
[26] O.Pana, Surface Science **601**, 4352 (2007).
[27] Marco Garza-Navarro, Journal of Solid State Chemistry **183,** 99 (2010).
[28] Yong Li, Materials Letters **60**, 750 (2006).
[29] Sukdeb Pal, APPLIED AND ENVIRONMENTAL MICROBIOLOGY, Mar. 2007, p. 1712–1720